

Analytical Description of the Dynamic Behaviour of the Passive Battery Supercapacitor Hybrid System

Dalibor BULJIĆ, Tomislav BARIĆ, Hrvoje GLAVAŠ*

Abstract: This paper presents a passive hybrid battery and supercapacitor system (HBSS). The load is modelled as a current sink. The waveform of the load current consists of rectangular pulses. The paper gives a mathematical model that accurately describes the HBSS behaviour during transient and steady state. In this paper, the approach using two introduced auxiliary parameters is applied in the analysis of the HBSS behaviour during transient and steady state. The introduced auxiliary parameters are functionally related to HBSS circuit parameters. All relevant expressions for voltages and currents are expressed through the introduced parameters. The influence of the electric circuit parameters on the voltages at HBSS terminals, battery and supercapacitor currents has been analysed in detail. The aim of the paper is to provide analytical expressions that establish the relations between the circuit parameters and their impact on voltages at HBSS terminals, battery and supercapacitor currents, as well as those analytical expressions that describe the HBSS behaviour during the transients. The expressions are presented in the form which allows a fast and easy application in the design and analysis of the presented HBSS.

Keywords: battery; hybrid battery supercapacitor system; supercapacitor; steady state; transients

1 INTRODUCTION

Batteries and supercapacitors (SCs), also known as ultracapacitors, as energy storage devices, store energy through different processes. Batteries store energy through a chemical process [1, 2], while SCs store energy through a charge separation process at the solid-liquid interface [3-8]. A distinctive difference between batteries and supercapacitors (SC) as energy storage devices is in the gravimetric power density and the gravimetric energy density [9-11]. Compared to batteries, SCs have a higher gravimetric power density and are better sources of power, i.e. they act as high power density energy storage devices, while batteries have a higher gravimetric energy density and are better for energy storage, i.e. they act as high energy density storage devices (Fig. 1. a compilation based on [9-11]).

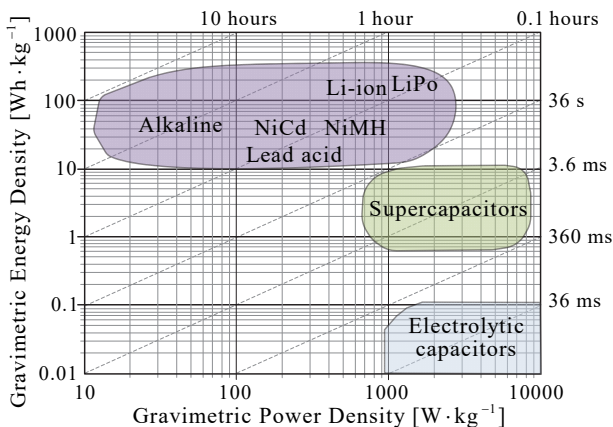


Figure 1 Ragone plot of selected energy storage technologies with charge/discharge time

These two diagonally opposite desirable properties of batteries and SCs can be used by combining the battery and the SC into one system. By combining the battery and the supercapacitor into one system, a hybrid battery-supercapacitor energy storage system is obtained [12-17]. The resulting hybrid energy storage system has desirable properties from both batteries and supercapacitors, i.e. high

gravimetric energy and power density. In addition to these obvious benefits, hybridisation of a battery and a supercapacitor in one system also brings a number of other benefits, briefly described as follows. In the case of a dynamic load, when the load current increases suddenly (abruptly), the voltage drop due to the dynamic component of the current at HBSS terminals is smaller than the voltage drop at the stand-alone battery terminals. During the dynamic component of the load current, the dynamic component of the current is distributed in the HBSS between the batteries and the SC. Initially, when a current pulse occurs, a larger part of the dynamic component of the load current is taken over by the SC [9, 18-22]. Both phenomena, the initial takeover of a larger part of the current pulse on the supercapacitor, and the distribution of the current pulse on the battery and the SC are beneficial.

Given that the battery heat losses are proportional to the square of the battery current, due to the reduced battery current in the HBSS during the current pulse, the battery heat losses are dramatically reduced. Because of the above, the overtemperature of the battery in the HBSS is lower than in the stand-alone battery under the same circumstances. Furthermore, the rate at which the battery temperature changes is lower, which reduces the thermal stress of the battery. A lower operating temperature of the battery and less thermal stress of the battery have a beneficial effect on battery life [22-24].

Given that the presence of SCs in the HBSS reduces battery losses under a dynamic load, the HBSS has greater energy efficiency compared to the stand-alone battery under the same conditions [9, 25-26]. The presence of SCs in the HBSS increases the peak power that the HBSS can deliver according to a consumer request. The reverse is also true; the ability to absorb power increases, which occurs during the braking of electric drives. Because of a number of benefits that battery-SC hybrid energy systems have in relation to individual systems based on batteries or SCs, numerous research studies on hybrid battery-SC energy systems have been conducted and different topologies have been developed (Fig. 2 a compilation based on [12-17, 27]).

The existing topologies of hybrid battery-SC energy systems can be categorised according to the number of components for energy storage, the method on which the power flows between them are based, and the structure. The simplest topology of hybrid battery-SC energy systems consists of a battery and a supercapacitor connected in parallel to common DC buses (Fig. 3. a compilation based on [12-17, 27]). Such a hybrid battery-SC energy system is called a passive hybrid battery-SC energy storage system (battery-SC HESS), or a passive hybrid battery and supercapacitor system (HBSS).

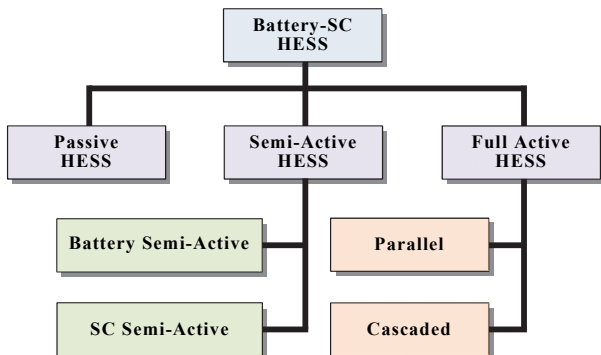


Figure 2 One of the classifications of the hybrid battery-supercapacitor topologies

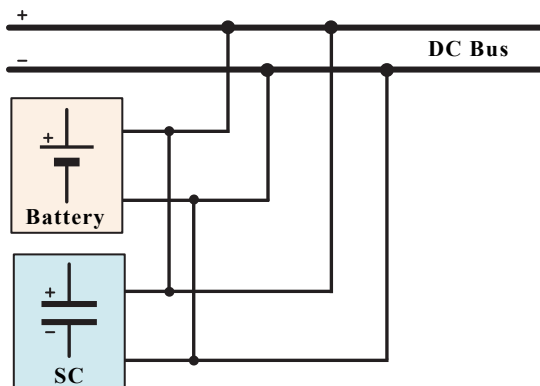


Figure 3 Topology of a passive battery-supercapacitor hybrid energy storage system

Power flows in such a system are determined by the battery and SC parameters. Once built, such a system does not have the possibility of changing its behaviour if the load characteristics change, or if the system parameters change due to aging or environmental influences such as temperature. In terms of the above, this type of system is designed in advance for a specific type of load characteristic. The lack of flexibility in operation can be overcome by using power electronics circuits [11, 14, 16]. By using power electronic circuits such as bidirectional power converters, power flows between HESS components can be managed within certain limits. Passive HBSS are widely used despite their simplicity and limitations compared to more advanced topologies. Given that the passive HBSS behaviour during transient and steady state is determined by HBSS circuit parameters, with the appropriate model it is possible to describe their behaviour with analytical expressions. There are numerous advantages of knowing analytical expressions that functionally relate circuit parameters to the system response.

By means of such analytical expressions, it is possible to establish an unambiguous relationship between circuit parameters and the desired response of the system. The above enables a quick procedure for designing a passive HBSS, i.e. determining the parameters of the supercapacitor and the battery for a specific desired response, i.e. the behaviour of the passive HBSS during transient and steady state. If there is a need for this, by conducting successive simulations for more complex battery and supercapacitor models, the required parameters of the battery and the supercapacitor can be determined more precisely. In this case, the values obtained by analytical expressions can be used for the initial values of more complex simulation models. Due to the above advantages brought by these types of analytical expressions, there is an abundance of analytical descriptions of the passive HBSS in the literature models [10, 18, 19, 21, 22, 26, 28, 29]. Analytical descriptions of the passive HBSS in the literature are obtained by variations of very simple HBSS models, different physical and mathematical approximations, and load models. This paper presents one of such approaches. The aim of the paper is to provide analytical expressions that establish the relations between the circuit parameters and their impact on voltages at HBSS terminals, battery and SC currents, and analytical expressions that describe the HBSS behaviour during the transients. The expressions are presented in the form which allows a fast and easy application in the design and analysis of the passive HBSS. In order for the physical assumptions and mathematical approximations under which the analytical expressions were obtained to be well defined and clear, the procedure for deriving the analytical expressions is presented in detail. Furthermore, numerous comments were made for the above during the process of obtaining analytical expressions.

2 VOLTAGE AT HBSS TERMINALS

A distinctive difference in the behaviour of stand-alone batteries and HBSS is the dynamic mode of operation. This is especially pronounced during sudden (sharp, rapid, step) changes in the load current. Without a supercapacitor, the battery-load circuit has a response that corresponds to a system without any significant inertia. The above is easiest to explain by comparing the voltage at HBSS terminals and the voltage at the terminals of the stand-alone battery for the same dynamic load. For this purpose, a rapidly changing dynamic load can be represented by the current pulse (Fig. 4). With a good assumption, a battery-load circuit can be considered a zero-order system, i.e. a system without inertia. Due to the voltage drop in the equivalent series resistance of the battery, any change in the current load will be instantly reflected on the voltage at the stand-alone battery terminals. For example, when the current pulse occurs (Fig. 4), the voltage at the stand-alone battery terminals will change abruptly (Fig. 4). The desired inertia is introduced into a system (HBSS) by hybridising the battery and the supercapacitor and due to the capacitance of the supercapacitor.

With a good assumption, a battery-supercapacitor-load circuit can be considered a first-order system. For the above, when the current pulse occurs (Fig. 4), the voltage at HBSS terminals will not change abruptly (Fig. 4).

In the steady state, before the current pulse occurs, current does not flow through the supercapacitor and the battery is loaded with a constant current of strength I_0 . Before the current pulse occurs, the battery terminal voltage U_0 is determined by the electromotive force (open circuit voltage U_{OC}) of the battery reduced by the voltage drop across the internal series resistance of the battery (R_B):

$$U_0 = E - I_0 \cdot R_B \quad (1)$$

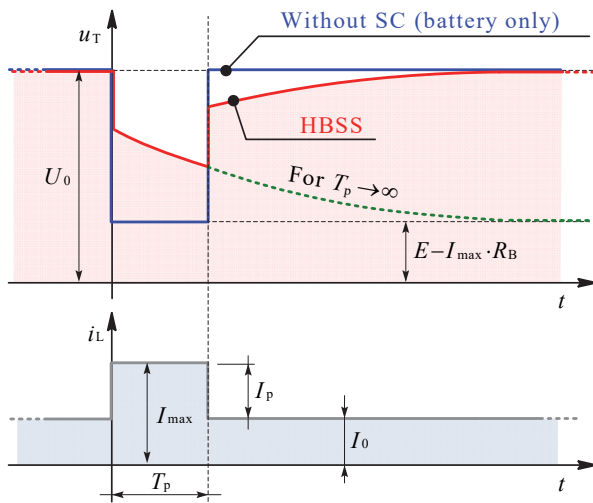


Figure 4 Wave forms of the load current and voltage at battery terminals without and with a supercapacitor

The dashed green curve in Fig. 4 represents the battery terminal voltage for a theoretical case in which the current pulse would still exist. In the model presented in this paper, it is assumed that the time interval between two consecutive current pulses is greater than the duration of the process of discharging and charging the supercapacitor, that is, the duration of both transients. A detailed description of the passive HBSS model and the procedure used to determine the waveforms shown in Fig. 4 will be presented and explained in detail in the next section of this paper.

3 BATTERY, SUPERCAPACITOR AND LOAD MODEL

In order to describe the transient behaviour of the passive HBSS with relatively simple analytical expressions, it is necessary to reduce the complexity of the entire system to the necessary minimum. For this purpose, this paper used a load, battery and supercapacitor model, which proved to be suitable according to the literature [10, 18, 19, 21, 22, 26-29].

3.1 Load Model

Load is modelled as a current sink (Fig. 5 [9, 11]) with such a current waveform that credibly represents the expected load. The current waveform includes a time interval of constant load for modelling a static load and sudden overloads for modelling a dynamic load.

For this purpose, the load current is most often presented in the literature as an algebraic sum of constant amplitude I_0 and a periodic pulse train with period T consisting of rectangular pulses of duration T_p and

amplitude I_p (Fig. 5 [9, 11]). The load current can be concisely written using unit step functions [9, 11]:

$$i_L = I_0 + \sum_{k=0}^N (I_p - I_0)(u(t - kT) - u(t - T_p - kT)) \quad (2)$$

where $u(t - kT)$ and $u(t - T_p - kT)$ are unit step functions.

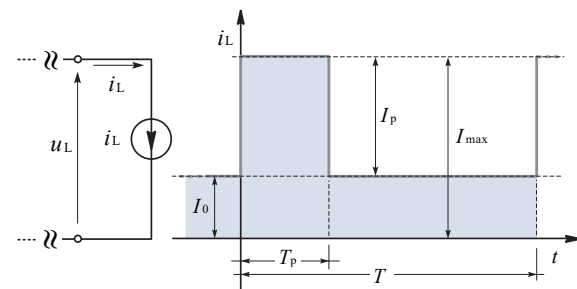


Figure 5 Load model and waveform of the load current with relevant quantities

3.2 Battery and Supercapacitor Model

The battery is modelled as a series connection of the electromotive force E (open circuit voltage U_{OC}) and the equivalent series resistance R_B . The SC is modelled as a series connection of the capacitance denoted by C and the equivalent series resistance denoted by R_C . A battery and an SC are connected in parallel to common DC buses, topologically called passive HBSS. (Fig. 6 [9, 11]). According to Fig. 6, the battery-supercapacitor-load circuit is a first-order model.

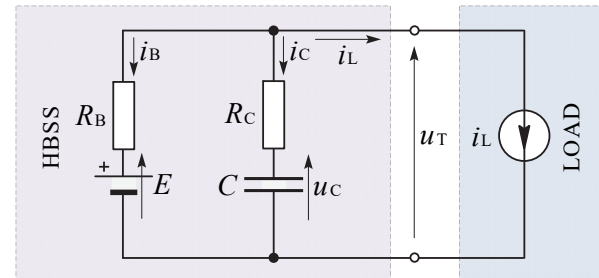


Figure 6 First-order model of the passive HBSS

4 MATHEMATICAL DESCRIPTION OF TRANSIENTS

This section describes in detail the procedure for obtaining the equations for the voltage and current transients within the passive HBSS shown in Fig. 6. Based on the circuit shown in Fig. 6, for each t the following holds:

$$i_L = -i_B - i_C \quad (3)$$

$$E + i_B \cdot R_B - i_C \cdot R_C - u_C = 0 \quad (4)$$

$$i_C = C \cdot \frac{du_C}{dt} \quad (5)$$

Voltage at HBSS terminals (corresponding to the load voltage u_L) is given by the expression:

$$u_T = u_C + i_C \cdot R_C \quad (6)$$

Combining Eq. (3) and Eq. (4) gives

$$E - i_L \cdot R_B - i_C \cdot (R_B + R_C) - u_C = 0 \quad (7)$$

Substitution of Eq. (5) into Eq. (7) gives

$$(R_B + R_C) \cdot C \cdot \frac{du_C}{dt} + u_C = E - i_L \cdot R_B \quad (8)$$

The previous expression can be written more concisely in the following form:

$$\tau \cdot \frac{du_C}{dt} + u_C = E - i_L \cdot R_B \quad (9)$$

where τ is the time constant determined by the expression:

$$\tau = (R_B + R_C) \cdot C \quad (10)$$

Eq. (9) can be recognised as a first-order differential equation. Differential Eq. (9) describes the discharging and charging transients of the SC. In both cases, time constant Eq. (10) remains unchanged. Depending on whether the SC is being charged or discharged, the change in Eq. (9) refers to the load current.

For the SC discharging process ($0_+ \leq t \leq T_p$):

$$i_L = I_0 + I_p \quad (11)$$

For the SC charging process ($T_p+ \leq t \leq T$):

$$i_L = I_0 \quad (12)$$

In order to differentiate the voltages for each individual process (charge or discharge), notations u_{C1} and u_{C2} will be used for the supercapacitor discharging process and the supercapacitor charging process, respectively. Moreover, the same subscript notation will be used to indicate the supercapacitor current during the supercapacitor discharging and charging process. The above also applies to other physical quantities, such as battery current and voltage at HBSS terminals. In accordance with the above, the general forms for voltage u_C can be written as follows:

$$u_C = \begin{cases} u_{C1} & \text{for } 0_+ \leq t \leq T_p-, \\ u_{C2} & \text{for } T_p+ \leq t \leq T. \end{cases} \quad (13)$$

4.1 Supercapacitor Discharging Process

For the SC discharging process ($0_+ \leq t \leq T_p$) the following holds:

$$\tau \cdot \frac{du_{C1}}{dt} + u_{C1} = E - (I_0 + I_p) \cdot R_B \quad (14)$$

According to the commutative law [30], immediately before commutation ($t = 0_-$) and immediately after

commutation ($t = 0_+$), i.e. immediately before and immediately after the current pulse occurs, the voltage u_{C1} remains unchanged:

$$u_{C1}(0_-) = u_{C1}(0_+) = E - i_L(0_-) \cdot R_B \quad (15)$$

Since $i_L(0_-) = I_0$, it follows that

$$u_{C1}(0_-) = u_{C1}(0_+) = E - I_0 \cdot R_B = U_0 \quad (16)$$

Applying the Laplace transform to Eq. (12) gives

$$\tau \cdot [s \cdot U_{C1}(s) - u_{C1}(0_-)] + U_{C1}(s) = \frac{E - (I_0 + I_p) \cdot R_B}{s} \quad (17)$$

Rearranging the previous expression gives

$$U_{C1}(s) = \frac{u_{C1}(0_-)}{s + \frac{1}{\tau}} + \frac{1}{T} \cdot \frac{1}{s} \cdot \frac{(E - (I_0 + I_p) \cdot R_B)}{s + \frac{1}{\tau}} \quad (18)$$

By introducing a substitute

$$\Delta U_p = I_p \cdot R_B \quad (19)$$

and taking into account (16), Eq. (18) can be simplified to the following form:

$$U_{C1}(s) = \frac{U_0}{s + \frac{1}{\tau}} + \frac{1}{\tau} \cdot \frac{1}{s} \cdot \frac{U_0 - \Delta U_p}{s + \frac{1}{\tau}} \quad (20)$$

The voltage drop ΔU_p has the physical meaning of the voltage drop across the battery that would occur due to the current I_p if there were no supercapacitor. Applying the inverse Laplace transform to Eq. (20), and after rearrangement, we obtain the following expression:

$$u_{C1} = U_0 - \Delta U_p \cdot \left(1 - e^{-\frac{t}{\tau}} \right) \quad (21)$$

The supercapacitor current during the discharging process is:

$$i_{C1} = C \cdot \frac{du_{C1}}{dt} = -\Delta U_p \cdot \frac{C}{\tau} e^{-\frac{t}{\tau}} = -\frac{\Delta U_p}{R_B + R_C} e^{-\frac{t}{\tau}} \quad (22)$$

Taking into account (19) yields:

$$i_{C1} = -I_p \frac{R_B}{R_B + R_C} e^{-\frac{t}{\tau}} \quad (23)$$

A negative sign of the current indicates that the actual direction of the current during the discharging process is opposite to the direction shown in Fig. 6. For the sake of more concise expressions and benefits that will be obvious later, the following substitutions were introduced:

$$k = \frac{R_B}{R_C} \quad (24)$$

$$K = K(k) = \frac{R_B}{R_B + R_C} = \frac{k}{1+k} \quad (25)$$

The dependence of the parameter K on the ratio $k = R_B / R_C$ is shown graphically in Fig. 7.

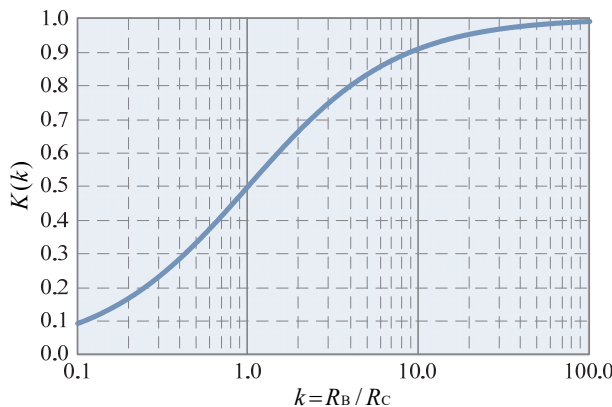


Figure 7 Dependence of the parameter K on the ratio k

By using the newly introduced substitutions, the expression for the supercapacitor current can be written in the form:

$$i_{C1} = -I_p \cdot K \cdot e^{-\frac{t}{\tau}} \quad (26)$$

It follows from Eq. (3) that

$$i_B = -i_L - i_C \quad (27)$$

By substituting Eq. (11) and Eq. (26) into Eq. (27), we obtain:

$$i_{B1} = -(I_0 + I_p) + I_p \cdot K \cdot e^{-\frac{t}{\tau}} = -I_0 - I_p \left(1 - K \cdot e^{-\frac{t}{\tau}} \right) \quad (28)$$

At this point, it is appropriate to comment on the impact of the supercapacitor on the reduction of the battery current in the passive HBSS. The influence of the SC on the reduction of the battery current during the current pulse can be analysed through the parameter K . If the resistances of the battery and the supercapacitor are equal ($k = 1$), according to Fig. 7, $K = 0.5$. Then exactly half of the current I_p from the current pulse was equally distributed to the battery and the supercapacitor.

As the ratio k increases above one, the parameter K becomes greater than 0.5, and a larger share of the pulse current I_p is taken over by the supercapacitor. By combining Eq. (6) and Eq. (23), we obtain the expression for voltage at HBSS terminals:

$$u_{T1} = U_0 - \Delta U_p \cdot \left(1 - e^{-\frac{t}{\tau}} \right) - I_p \frac{R_B \cdot R_C}{R_B + R_C} e^{-\frac{t}{\tau}} \quad (29)$$

Taking into account (19) yields

$$u_{T1} = U_0 - \Delta U_p \cdot \left(1 - e^{-\frac{t}{\tau}} \right) - \Delta U_p \cdot \frac{R_C}{R_B + R_C} e^{-\frac{t}{\tau}} \quad (30)$$

The previous expression can be further simplified if the following dependence is recognised:

$$\frac{R_C}{R_C + R_B} = \frac{1}{R_C} \frac{R_C}{1 + \frac{R_B}{R_C}} = \frac{1}{1+k} \quad (31)$$

Combining Eq. (30) and Eq. (31) gives

$$u_{T1} = U_0 - \Delta U_p \cdot \left(1 - e^{-\frac{t}{\tau}} \right) - \Delta U_p \frac{1}{1+k} e^{-\frac{t}{\tau}} \quad (32)$$

Rearranging the terms in the previous expression yields

$$u_{T1} = U_0 - \Delta U_p \cdot \left(1 + \left(\frac{1}{1+k} - 1 \right) e^{-\frac{t}{\tau}} \right) \quad (33)$$

i.e., after minor editing, we obtain:

$$u_{T1} = U_0 - \Delta U_p \cdot \left(1 - \frac{k}{1+k} e^{-\frac{t}{\tau}} \right) \quad (34)$$

Taking into account (25), voltage at HBSS terminals can be written more concisely as follows:

$$u_{T1} = U_0 - \Delta U_p \cdot \left(1 - K \cdot e^{-\frac{t}{\tau}} \right) \quad (35)$$

An instantaneous voltage drop at HBSS terminals at the occurrence of the current pulse I_p is determined on the basis of the expression:

$$\Delta U_i = u_{T1}(0_-) - u_{T1}(0_+) \quad (36)$$

Voltage at HBSS terminals before the occurrence of the current pulse ($t=0_-$) is equal to the voltage in the steady state:

$$u_{T1}(0_-) = u_{C1}(0_-) = U_0 \quad (37)$$

Voltage at HBSS terminals immediately after the occurrence of the current pulse ($t=0_+$) is determined by Eq. (35). Substituting $t=0_+$ into Eq. (35) gives

$$u_{T1}(0_+) = U_0 - \Delta U_p \cdot (1 - K) \quad (38)$$

Inserting Eq. (37) and Eq. (38) into Eq. (36) gives an expression for the instantaneous voltage drop at HBSS terminals:

$$\Delta U_i = u_{T1}(0_-) - u_{T1}(0_+) = \Delta U_p \cdot (1 - K) \quad (39)$$

In addition, it is interesting to know the voltage drop at HBSS terminals during the transient that occurs after the instantaneous voltage drop at HBSS terminals. This voltage drop develops gradually (without a sudden jump), and it is determined by the following expression:

$$\Delta U_t = u_{T1}(0_+) - u_{T1}(T_p) \quad (40)$$

Voltage at HBSS terminals at $t = T_p$ is determined by Eq. (35) and reads:

$$u_{T1}(T_p) = U_0 - \Delta U_p \cdot \left(1 - K \cdot e^{-\frac{T_p}{\tau}}\right) \quad (41)$$

Voltage at HBSS terminals immediately after the occurrence of the current pulse ($t = 0_+$) is given by Eq. (38). By substituting Eq. (38) and Eq. (41) into Eq. (40) gives an expression for the transient voltage drop at HBSS terminals:

$$\begin{aligned} \Delta U_t &= \Delta U_p \cdot \left(1 - K \cdot e^{-\frac{T_p}{\tau}}\right) - \Delta U_p \cdot (1 - K) = \\ &= \Delta U_p \cdot K \cdot e^{-\frac{T_p}{\tau}}. \end{aligned} \quad (42)$$

On the basis of previously derived analytical expressions, it is possible to construct a qualitative voltage waveform at HBSS terminals during the SC discharging process (Fig. 8).

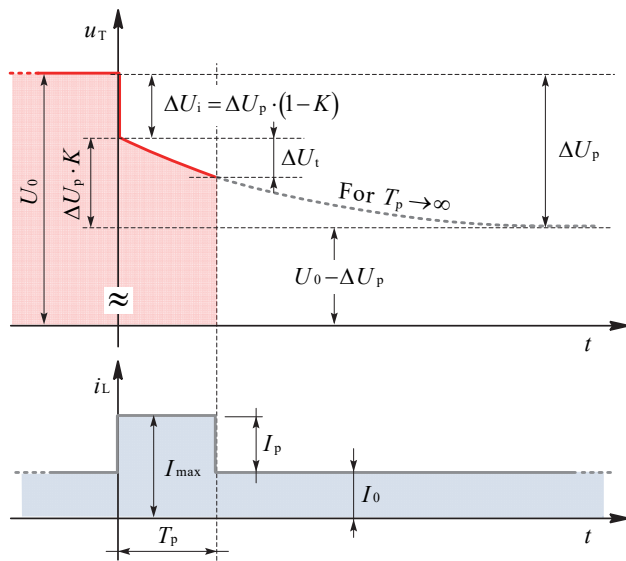


Figure 8 Waveforms of the load current and voltage at HBSS terminals with relevant physical quantities during the supercapacitor discharging process

It will be possible to qualitatively construct the remaining part of the voltage waveform at HBSS terminals after the analysis of the supercapacitor charging process.

4.2 Supercapacitor Charging Process

For the SC charging process ($T_p \leq t \leq T$) it holds:

$$\tau \cdot \frac{du_{C2}}{dt} + u_{C2} = E - I_0 \cdot R_B \quad (43)$$

Taking into account (1), the previous expression can be written as follows:

$$\tau \cdot \frac{du_{C2}}{dt} + u_{C2} = U_0 \quad (44)$$

According to the commutative law [30], immediately before commutation ($u_{C2}(T_p_-)$) and immediately after commutation ($u_{C2}(T_p_+)$), the voltage u_{C2} remains unchanged:

$$u_{C2}(T_p_-) = u_{C2}(T_p_+) = u_{C1}(T_p) = U_0 - \Delta U_p \cdot \left(1 - e^{-\frac{T_p}{\tau}}\right) \quad (45)$$

The solution to differential Eq. (44) is obtained by taking into account initial condition (45) and applying the procedure described in Eqs. (14)-(21):

$$u_{C2} = u_{C1}(T_p) + (U_0 - u_{C1}(T_p)) \cdot \left(1 - e^{-\frac{t-T_p}{\tau}}\right) \quad (46)$$

The supercapacitor current during the charging process is:

$$i_{C2} = C \cdot \frac{du_{C2}}{dt} = (U_0 - u_{C1}(T_p)) \cdot \frac{C}{\tau} \cdot e^{-\frac{t-T_p}{\tau}} \quad (47)$$

By substituting Eq. (10) into the previous expression, we obtain:

$$i_{C2} = \frac{U_0 - u_{C1}(T_p)}{R_B + R_C} \cdot e^{-\frac{t-T_p}{\tau}} \quad (48)$$

Taking into account the introduced notation, it follows from Eq. (6) that

$$u_{T2} = u_{C2} + i_{C2} \cdot R_C \quad (49)$$

By substituting Eq. (46) and Eq. (48) into the previous expression, we obtain:

$$\begin{aligned} u_{T2} &= u_{C1}(T_p) + (U_0 - u_{C1}(T_p)) \cdot \left(1 - e^{-\frac{t-T_p}{\tau}}\right) + \\ &\quad + (U_0 - u_{C1}(T_p)) \cdot \frac{R_C}{R_B + R_C} \cdot e^{-\frac{t-T_p}{\tau}} \end{aligned} \quad (50)$$

Taking into account (31) yields

$$u_{T2} = u_{C1}(T_p) + (U_0 - u_{C1}(T_p)) \cdot \left(1 + \left(\frac{1}{1+k} - 1 \right) \cdot e^{-\frac{t-T_p}{\tau}} \right) \quad (51)$$

After minor editing of the previous expression we obtain:

$$u_{T2} = u_{C1}(T_p) + (U_0 - u_{C1}(T_p)) \cdot \left(1 - \frac{k}{1+k} \cdot e^{-\frac{t-T_p}{\tau}} \right) \quad (52)$$

Taking into account (25) yields

$$u_{T2} = u_{C1}(T_p) + (U_0 - u_{C1}(T_p)) \cdot \left(1 - K \cdot e^{-\frac{t-T_p}{\tau}} \right) \quad (53)$$

An instantaneous voltage jump at HBSS terminals after the disappearance of the current pulse I_p is determined on the basis of the expression:

$$\Delta U'_t = u_{T2}(T_p+) - u_{T1}(T_p-) \quad (54)$$

Voltage at HBSS terminals immediately after the disappearance of the current pulse ($t = T_p+$) is determined by Eq. (53):

$$u_{T2}(T_p+) = u_{C1}(T_p) + (U_0 - u_{C1}(T_p)) \cdot (1 - K) \quad (55)$$

Voltage at HBSS terminals immediately before the disappearance of the current pulse ($t = T_p-$) is determined by the Eq. (41).

$$u_{T1}(T_p-) = U_0 - \Delta U_p \cdot \left(1 - K \cdot e^{-\frac{T_p}{\tau}} \right) \quad (56)$$

Inserting Eq. (55) and Eq. (56) into Eq. (54) gives an expression for the instantaneous voltage jump at HBSS terminals after the disappearance of the current pulse I_p :

$$\begin{aligned} \Delta U'_t &= u_{T2}(T_p+) - u_{T1}(T_p-) = \\ &= u_{C1}(T_p) + (U_0 - u_{C1}(T_p)) \cdot (1 - K) - \\ &- U_0 - \Delta U_p \cdot \left(1 - K \cdot e^{-\frac{T_p}{\tau}} \right). \end{aligned} \quad (57)$$

Based on the derived expressions for the voltage at the HBSS terminals, it is possible to graphically represent the general appearance of the waveform of the terminal voltage of the HBSS (Fig.9).

The waveform of the voltage at HBSS terminals shown in Fig. 9 is consistent with the results in the literature obtained by measurements and simulations [10, 11, 21, 31-33].

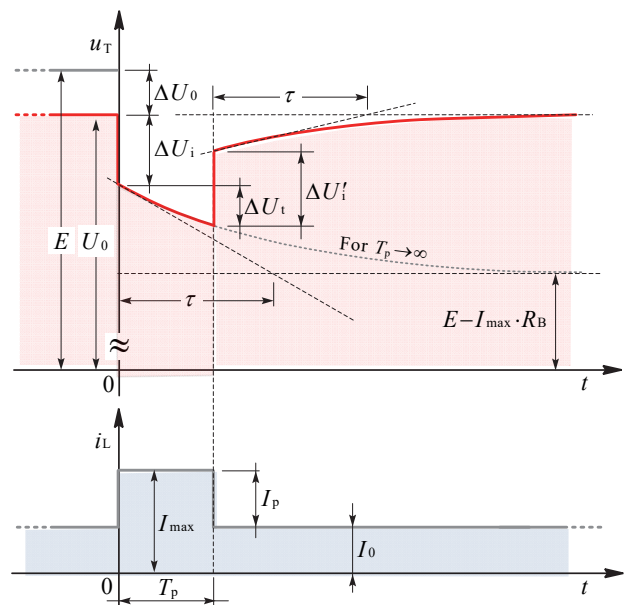


Figure 9 Waveforms of the load current and voltage at HBSS terminals with relevant physical quantities

4.3 Battery Current in the HBSS

In the previously presented theory, it was shown that the presence of supercapacitors has a beneficial effect on the voltage at HBSS terminals. Due to the presence of the supercapacitor, the voltage at HBSS terminals has a significantly smaller drop when the current pulse occurs. Another benefit of the presence of supercapacitors in the HBSS refers to battery current. Due to the presence of the supercapacitor, battery current is significantly lower during the occurrence of the current pulse. Using the introduced notation for the time interval $0 \leq t \leq T$, battery and load currents can be written as follows:

$$i_B = \begin{cases} i_{B1} & \text{for } 0_+ \leq t \leq T_p-, \\ i_{B2} & \text{for } T_p+ \leq t \leq T. \end{cases} \quad (58)$$

$$i_L = \begin{cases} I_0 + I_p & \text{for } 0_+ \leq t \leq T_p-, \\ I_0 & \text{for } T_p+ \leq t \leq T. \end{cases} \quad (59)$$

Combining the previous two expressions yields

$$i_B = \begin{cases} -(I_0 + I_p) - i_{C1} & \text{for } 0_+ \leq t \leq T_p-, \\ -I_0 - i_{C2} & \text{for } T_p+ \leq t \leq T. \end{cases} \quad (60)$$

Currents i_{C1} and i_{C2} are determined by Eq. (26) and Eq. (48) and read as follows:

$$i_{C1} = -I_p \cdot K \cdot e^{-\frac{t}{\tau}} \quad (61)$$

$$i_{C2} = \frac{U_0 - u_{C1}(T_p)}{R_B + R_C} \cdot e^{-\frac{t-T_p}{\tau}} \quad (62)$$

For further convenience, it is preferable to express the current i_{C2} via the parameter K . It follows from Eq. (25) that

$$\frac{1}{R_B + R_C} = \frac{K}{R_B} \quad (63)$$

Combining Eq. (62) and Eq. (63) yields

$$i_{C2} = \frac{U_0 - u_{C1}(T_p)}{R_B + R_C} \cdot e^{-\frac{t-T_p}{T}} = \frac{K}{R_B} \cdot (U_0 - u_{C1}(T_p)) \cdot e^{-\frac{t-T_p}{T}} \quad (64)$$

From Eq. (21), it follows that

$$u_{C1}(T_p) = U_0 - \Delta U_p \cdot \left(1 - e^{-\frac{T_p}{\tau}}\right) \quad (65)$$

Combining Eq. (64) and Eq. (65) yields

$$i_{C2} = \frac{K}{R_B} \cdot \Delta U_p \cdot \left(1 - e^{-\frac{T_p}{\tau}}\right) \cdot e^{-\frac{t-T_p}{T}} \quad (66)$$

Given that $\Delta U_p = I_p \cdot R_B$, the previous expression can be written in the following form:

$$i_{C2} = I_p \cdot K \cdot \left(1 - e^{-\frac{T_p}{\tau}}\right) \cdot e^{-\frac{t-T_p}{T}} \quad (67)$$

Inserting Eq. (61) and Eq. (67) into Eq. (60) gives the currents i_{B1} and i_{B2} expressed by using the parameter K :

$$i_{B1} = -I_0 - I_p \cdot \left(1 - K \cdot e^{-\frac{t}{\tau}}\right) \quad (68)$$

$$i_{B2} = -I_0 - i_{C2} = -I_0 - I_p \cdot K \cdot \left(1 - e^{-\frac{T_p}{\tau}}\right) \cdot e^{-\frac{t-T_p}{\tau}} \quad (69)$$

When the current pulse occurs ($t = 0_+$), there is an instant change in the supercapacitor and battery currents.

$$\Delta i_C = i_C(0_+) - i_C(0_-) = \Delta i_{C1} = I_p \cdot K \quad (70)$$

$$\Delta i_B = i_B(0_+) - i_B(0_-) = I_p \cdot (1 - K) \quad (71)$$

During the current pulse, the supercapacitor current decreases and the current of the battery increases. The moment immediately before the end of the current pulse ($t = T_p^-$), according to Eqs. (61) and (68), the absolute values of the supercapacitor and battery currents are as follows:

$$|i_C(T_p^-)| = |i_{C1}(T_p^-)| = I_p \cdot K \cdot e^{-\frac{T_p}{\tau}} \quad (72)$$

$$|i_B(T_p^-)| = |i_{B1}(T_p^-)| = I_0 + I_p \cdot \left(1 - K \cdot e^{-\frac{T_p}{\tau}}\right) \quad (73)$$

An instantaneous battery current drop after the disappearance of the current pulse ($t = T_p^+$) is determined by expression (69):

$$\Delta i_B = I_p \cdot K \cdot \left(1 - e^{-\frac{T_p}{\tau}}\right) \quad (74)$$

An instantaneous change in the direction of the supercapacitor current after the disappearance of the current pulse ($t = T_p^+$) is determined by expression (67):

$$i_C(T_p^+) = i_{C2}(T_p^+) = I_p \cdot K \cdot \left(1 - e^{-\frac{T_p}{\tau}}\right) \quad (75)$$

Expressing the currents i_{C1} and i_{C2} , and the currents i_{B1} and i_{B2} by using the K parameter enables a qualitative graphical representation of the waveform of all HBSS currents (Fig. 10). The battery and supercapacitor current waveforms shown in Fig. 10 are consistent with the simulation results shown in [10, 11, 21, 31-34].

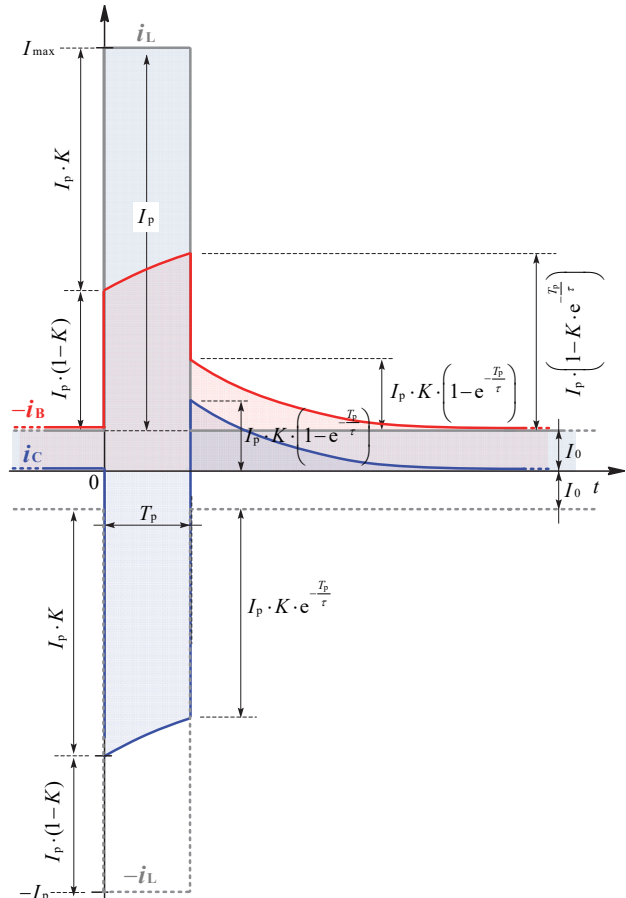


Figure 10 Waveforms of the load, battery and supercapacitor current and relevant physical quantities

5 CONCLUSION

Batteries and supercapacitors as energy storage devices have certain mutually distinctive characteristics. Batteries have a higher gravimetric energy density, approximately an order of magnitude higher than

supercapacitors, while supercapacitors have a higher gravimetric power density, approximately an order of magnitude higher than batteries.

By combining supercapacitors and batteries into one system (HBSS), the specific and desirable characteristics of each of these energy storage devices can be exploited. In addition to the above, the hybrid battery and supercapacitor system also have numerous other desirable characteristics that a stand-alone battery does not have under a dynamic load, e.g. reduced dynamic component of the battery current in the passive HBSS compared to a stand-alone battery, reduced losses in the battery as an HBSS component compared to a stand-alone battery, reduced total losses in the HBSS compared to a stand-alone battery, reduced battery heating in the passive HBSS compared to a stand-alone battery, reduced battery thermal stress, improved energy efficiency, and the voltage at the passive HBSS terminals does not change abruptly when the load current changes abruptly. The physical reasons for the aforementioned advantages of the passive HBSS compared to a stand-alone battery are described in detail in this paper. The paper contains all necessary analytical expressions that characterise the voltage waveform at the passive HBSS terminals under a dynamic load. In addition, all necessary expressions are given that characterise the battery current in the passive HBSS during a dynamic load.

The derived expressions are brought into a form that is described by the two parameters introduced that are related to circuit parameters. Because of the above, the presented analytical expressions can be easily applied practically when determining the necessary circuit parameters for the desired response of the passive HBSS to a specific dynamic load. Furthermore, if it is necessary to model the passive HBSS with a more complex model and analyse its operation through simulations, then the derived expressions can be used to obtain the initial values of a more complex simulation model.

6 REFERENCES

- [1] Linden, D. & Reddy, T. (2001). *Handbook of Batteries*. McGraw Hill Professional. 3rd edition, ISBN-10: 0-07-135978-8.
- [2] Plett, G. L. (2020). *Battery Management Systems, Volume II: Equivalent-Circuit Methods*. Artech House. 2nd edition, ISBN-13: 978-1-63081-027-6.
- [3] Beguin, F., Frackowiak, E. & Lu M. (2013). *Supercapacitors: Materials, Systems, and Applications*. Wiley-VCH.
- [4] Yu, A., Chabot, V., & Zhang, J. (2017). *Electrochemical Supercapacitors for Energy Storage and Delivery: Fundamentals and Applications*. CRC Press.
- [5] Miller, J. M. (2011). *Ultracapacitor Applications*. IET.
- [6] Conway, B. E. (2013). *Electrochemical Supercapacitors: Scientific Fundamentals and Technological Applications*. Springer Science & Business Media.
- [7] Deshpande, R. (2015). *Ultracapacitors*. McGraw-Hill Education.
- [8] Kötz, R. & Carlen, M. (2000). Principles and applications of electrochemical capacitors. *Electrochimica Acta*, 45(15-16), 2483-2498. [https://doi.org/10.1016/s0013-4686\(00\)00354-6](https://doi.org/10.1016/s0013-4686(00)00354-6)
- [9] Kuperman, A. & Aharon, I. (2011). Battery–ultracapacitor hybrids for pulsed current loads: A review. *Renewable & Sustainable Energy Reviews*, 15(2), 981-992. <https://doi.org/10.1016/j.rser.2010.11.010>
- [10] Ma, T., Yang, H., & Lu, L. (2015). Development of hybrid battery-supercapacitor energy storage for remote area renewable energy systems. *Applied Energy*, 153, 56-62. <https://doi.org/10.1016/j.apenergy.2014.12.008>
- [11] Seim, L. H. (2012). Modeling, control and experimental testing of a supercapacitor/battery hybrid system: passive and semi-active topologies. *147*.
- [12] Wang, E., Yang, F., & Ouyang, M. (2017). A hybrid energy storage system for a coaxial power-split hybrid powertrain. *InTech eBooks*. <https://doi.org/10.5772/67756>
- [13] Mi, C., Masrur, M. A., & Gao, D. W. (2011). *Hybrid electric vehicles: Principles and Applications with Practical Perspectives*. Wiley.
- [14] Cabrane, Z., Ouassaid, M., & Maâroufi, M. (2016). Analysis and evaluation of battery-supercapacitor hybrid energy storage system for photovoltaic installation. *International Journal of Hydrogen Energy*, 41(45), 20897-20907. <https://doi.org/10.1016/j.ijhydene.2016.06.141>
- [15] Dong, Z., Zhang, Z., Li, Z., Li, X., Qin, J., Liang, C., Han, M., Yin, Y., Bai, J., Wang, C., & Wang, R. (2022). A survey of Battery-Supercapacitor Hybrid Energy Storage Systems: Concept, Topology, control and Application. *Symmetry*, 14(6), 1085. <https://doi.org/10.3390/sym14061085>
- [16] Jing, W., Lai, C. H., Wong, S. H. W., & Wong, M. L. D. (2017). Battery-supercapacitor hybrid energy storage system in standalone DC microgrids: areview. *IET Renewable Power Generation*, 11(4), 461-469. <https://doi.org/10.1049/iet-rpg.2016.0500>
- [17] Jayasawal, K., Karna, A. K., & Thapa, K. B. (2021). Topologies for interfacing supercapacitor and battery in hybrid electric vehicle applications: An overview. *2021 International Conference on Sustainable Energy and Future Electric Transportation (SEFET)*. <https://doi.org/10.1109/sefet48154.2021.9375802>
- [18] Bolborici, V., Dawson, F. P., & Lian, K. K. (2011). Sizing considerations for ultracapacitors in hybrid energy storage systems. *2011 IEEE Energy Conversion Congress and Exposition*. <https://doi.org/10.1109/ecce.2011.6064159>
- [19] Hanmin, L., Zhixin, W., Jie, C., & Maly, D. (2009, March). Improvement on the Cold Cranking Capacity of Commercial Vehicle by Using Supercapacitor and Lead-Acid Battery Hybrid. *IEEE Transactions on Vehicular Technology*, 58(3), 1097-1105. <https://doi.org/10.1109/tvt.2008.929220>
- [20] Lahbib, I., Lahyani, A., Sari, A., & Venet, P. (2014, March). Performance analysis of a lead-acid battery/supercapacitors hybrid and a battery stand-alone under pulsed loads. *2014 First International Conference on Green Energy ICGE 2014*. <https://doi.org/10.1109/icge.2014.6835434>
- [21] Gu, G., Lao, Y., Ji, Y., Yuan, S., Liu, H., & Du, P. (2023). Development of hybrid super-capacitor and lead-acid battery power storage systems. *International Journal of Low-Carbon Technologies*, 18, 159-166. <https://doi.org/10.1093/ijlct/ctac140>
- [22] Dougal, R., Liu, S., & White, R. (2002, March). Power and life extension of battery-ultracapacitor hybrids. *IEEE Transactions on Components and Packaging Technologies*, 25(1), 120-131. <https://doi.org/10.1109/6144.991184>
- [23] Tshiani, C. T. & Umenne, P. (2022). The Impact of the Electric Double-Layer Capacitor (EDLC) in Reducing Stress and Improving Battery Lifespan in a Hybrid Energy Storage System (HESS) System. *Energies*, 15(22), 8680. <https://doi.org/10.3390/en15228680>
- [24] Shin, D., Poncino, M., & Macii, E. (2014). Thermal management of batteries using a hybrid supercapacitor architecture. *Design, Automation & Test in Europe Conference & Exhibition (DATE), 2014*. <https://doi.org/10.7873/date.2014.344>
- [25] Pay, S. & Baghzouz, Y. Effectiveness of battery-supercapacitor combination in electric vehicles. *2003 IEEE Bologna Power Tech Conference Proceedings*.

- <https://doi.org/10.1109/ptc.2003.1304472>
- [26] Penella, M. & Gasulla, M. (2010, April). Runtime Extension of Low-Power Wireless Sensor Nodes Using Hybrid-Storage Units. *IEEE Transactions on Instrumentation and Measurement*, 59(4), 857-865.
<https://doi.org/10.1109/tim.2009.2026603>
- [27] Jing, W., Lai, C. H., Wong, W. S., & Wong, M. D. (2018, August). A comprehensive study of battery-supercapacitor hybrid energy storage system for standalone PV power system in rural electrification. *Applied Energy*, 224, 340-356. <https://doi.org/10.1016/j.apenergy.2018.04.106>
- [28] Naderi, E., K. C., B., Ansari, M., & Asrari, A. (2021, September). Experimental Validation of a Hybrid Storage Framework to Cope with Fluctuating Power of Hybrid Renewable Energy-Based Systems. *IEEE Transactions on Energy Conversion*, 36(3), 1991-2001.
<https://doi.org/10.1109/tec.2021.3058550>
- [29] Stienecker, A. W., Stuart, T., & Ashtiani, C. (2006, June). An ultracapacitor circuit for reducing sulfation in lead acid batteries for mild hybrid electric vehicles. *Journal of Power Sources*, 156(2), 755-762.
<https://doi.org/10.1016/j.jpowsour.2005.06.014>
- [30] Shenkman, A. L. (2006). *Transient Analysis of Electric Power Circuits Handbook*. Springer Science & Business Media.
- [31] Chuan, Y., Mi, C., & Zhang, M. (2012, March 30). Comparative Study of a Passive Hybrid Energy Storage System Using Lithium Ion Battery and Ultracapacitor. *World Electric Vehicle Journal*, 5(1), 83-90.
<https://doi.org/10.3390/wevj5010083>
- [32] Cericola, D. & Kötz, R. (2012, June). Hybridization of rechargeable batteries and electrochemical capacitors: Principles and limits. *Electrochimica Acta*, 72, 1-17.
<https://doi.org/10.1016/j.electacta.2012.03.151>
- [33] Stienecker, A. W., Stuart, T., & Ashtiani, C. (2006). An ultracapacitor circuit for reducing sulfation in lead acid batteries for Mild Hybrid Electric Vehicles. *Journal of Power Sources*, 156(2), 755-762.
<https://doi.org/10.1016/j.jpowsour.2005.06.014>
- [34] Turner, G. A. (2000). *US6836097B2 - Power supply for a pulsed load - Google Patents*. <https://patents.google.com/patent/US6836097B2/en>

Contact information:

Dalibor BULJIĆ, PhD Student
 Faculty of Electrical Engineering,
 Computer Science and Information Technology Osijek,
 University of Osijek,
 Kneza Trpimira 2B, 31000 Osijek, Croatia
 E-mail: dalibor.buljic@ferit.hr

Tomislav BARIĆ, PhD, Full Professor
 Faculty of Electrical Engineering,
 Computer Science and Information Technology Osijek,
 University of Osijek,
 Kneza Trpimira 2B, 31000 Osijek, Croatia
 E-mail: tomislav.baric@ferit.hr

Hrvoje GLAVAŠ, PhD, Full Professor
 (Corresponding author)
 Faculty of Electrical Engineering,
 Computer Science and Information Technology Osijek,
 University of Osijek,
 Kneza Trpimira 2B, 31000 Osijek, Croatia
 E-mail: hrvoje.glavas@ferit.hr